

Optimum Design for an Air Current Pulverizing Blade Using the Computational Fluid Dynamics

Gun-hoi Kim^{*,#}, Han-bit Kim^{*}

^{*}Department of Mechanical & Automotive Engineering, Jeonju University

CFD분석을 통한 기류식 분쇄기 날개부의 최적설계

김건희^{*,#}, 김한빛^{*}

^{*}전주대학교 기계자동차공학과

(Received 14 July 2020; received in revised form 21 July 2020; accepted 03 August 2020)

ABSTRACT

In the air current pulverizing type grinding method, the blade wings fitted inside a casing are rotated at a high speed to generate a cornering air current, which facilitates the collision of materials with one another, leading to the pulverizing phenomenon. In contrast to mechanical grinding, grit pulverizing leads to fine grinding and less acid waste and degeneration of the material. Moreover, this approach prevents the loss of nutritional value, while allowing the milling grain to have an excellent texture. However, the existing air current pulverizing type machines consist of prefabricated blades, which cannot be rotated at a speed higher than 5,000 rpm. Consequently, the grinding process becomes time consuming with a low productivity. To overcome these problems, in this study, the shape and structure of the air current pulverizing type wings were optimized to allow rapid grinding at more than 8,000 rpm. Moreover, the optimal design for the ripening parts for the air current pulverizing type device was determined by performing a computational fluid dynamics analysis based on airflow analyses to produce machinery that can grinding materials to the order of micrometers.

Keywords : Air Current Crushing(기류분쇄), Crushing Blade(분쇄 날), Computational Fluid Dynamics Analysis(CFD 해석), Optimum Design(최적설계), Micro-crushing Grit(미분입자)

1. Introduction

This study discusses the optimal wing shape design in an air current pulverizing blade that is designed to finely grinding objects to be pulverized

to a particle size as small as 3 μm . The air current pulverizing blade is composed of a pulverizing portion that integrates a rotating blade to increase the rotating speed of the pulverizing portion up to 8,000 revolutions per minute (RPM) by fixing the rotating axis and blade into an integrated shape.

Generally, “pulverizer” refers to a mechanical device that grinds solid-state materials into powder;

Corresponding Author : gunhoi@jj.ac.kr

Tel: +82-63-220-2997, Fax: +82-63-220-2995

they are widely employed in various industrial fields. The air current pulverizers in this study are classified as coarse crushers, intermediate crushers, or fine grinders according to the size of the materials to be pulverized, and into wet- and dry-type pulverizers according to the pulverizing condition^[1-2].

There are two methods of pulverizing grains: impact grinding method that applies mechanical impact and a freezing grinding method that makes materials sufficiently brittle through use of a refrigerant such as liquid nitrogen^[1-2]. The impact grinding method has drawbacks that the heat generated by the impacts degrades the quality of pulverized grains and grains with high oil content are poorly pulverized because of the deformation of grains by oil. The freezing grinding method requires expensive liquid nitrogen and pulverizers that use this method should be kept cool, which increases the installation and operation costs.

Air current pulverizing methods have been developed and used to solve the above problems. The air current pulverizing method in this study generates a swirling airflow by rotating grinding wings inside the casing at high speed and pulverizes materials with the swirling airflow as material particles collide with one another. The air current pulverizing method can prevent heat generation by minimizing the impulse so that materials with high oil content can be efficiently pulverized and installation investment cost and operation cost are less than the freezing grinding method. It can also grind grains finely compared to mechanical milling methods, has less acidification or spoiling—thus preventing any loss of nutrients—and pulverized grains can excellently preserve food texture.

However, conventional airflow pulverizers have the drawback that they cannot rotate pulverizing wings at >5,000 rpm because the wings are structured by the assembly. Accordingly, they have a limitation to finely grind grains and take significant time to grind, which reduces their productivity.

Thus, this study aimed to devise a shape and structure of pulverizing wings to overcome the limitation. For this, this study investigated the optimal vane shape design for air current pulverizing based on computational fluid dynamics (CFD) through airflow analysis to manufacture a mechanical device that can increase production and pulverize objects up to several μm in particle size due to the high-speed pulverization of > 8,000 rpm.

2. Optimum Design of Pulverizing Wing

2.1 CFD Analysis

CFD discretized the Navier–Stokes equations, which are nonlinear partial differential equations that describe fluid phenomena, using methods such as the finite difference method (FDM), finite element method (FEM), and finite volume method (FVM), thereby converting the Navier–Stokes equations into algebraic equations to solve and interpret fluid flow problems by employing numerical techniques and algorithms^[3].

2.1.1 Governing equation

Most flow analyses are solved based on the Navier–Stokes equations. Fluid flow is governed by the equation of continuity, which is a fundamental equation in fluid dynamics, and the Navier–Stokes equation. Equation (1) is induced from the mass conservation law for the equation of continuity and from the momentum conservation law for the Navier–Stokes equation^[4].

$$\frac{\partial}{\partial t}(\rho u) + \nabla \cdot (\rho u \otimes u + pI) = \nabla \tau + \rho g \quad (1)$$

u: Fluid speed, g: Gravitational acceleration, ρ : Density, p: Pressure, μ : Viscosity coefficient, ν : Value of dividing viscosity coefficient by density, ω : Value of dividing pressure by density, I: Unit matrix, \otimes : Tensor product

The above equation is arranged as follows by solving it using the Navier–Stokes equation regarding the fluid in this experiment as a non-viscous and incompressible flow. The above equation can be expressed by Eq. (2)^[4].

$$\frac{\partial u}{\partial t} + (u \cdot \nabla)u = -\nabla w + g \quad (2)$$

2.1.2 Boundary conditions for analysis

Three boundary conditions were used to set up the boundary condition for analysis. Dirichlet–Neumann boundary conditions were used to analyze the wall surface of the case in the airflow pulverizer and a periodic boundary condition was used for the axis and grinding wings, which were rotating bodies.

The Dirichlet boundary condition designates a value where a function should be performed along the domain boundary; this equation can be expressed by Eq. (3).

$$u(x) = a \quad (3)$$

When the fluid speed is designated as the above equation, a specific value a can be designated in the boundary of the function.

The Neumann boundary condition assigns a gradient value of the function in the boundary; this equation can be expressed by Eq. (4).

$$\frac{\partial u}{\partial x} = a \quad (4)$$

As presented in the above equation, a specific value a can be designated to the gradient of the function^[5–7].

The periodic boundary condition assumes that particles that are driven out of the calculation plane are reintroduced from the opposite side as the repeating periodic plane is divided. A single passage

of the axis or centrifugal turbomachine can be modeled using the periodic boundary condition (cyclic symmetry); this method captures the flow inside the blade passage although it is not the implementation of sliding mesh. The periodic boundary condition can also be used to simulate non-rotating devices^[8].

2.1.3 Numerical discretization method

The analytical solution of the numerical discretization Navier–Stokes equation can only be obtained for simple flows with ideal conditions.

The numerical analysis method converts a three-dimensional (3D) non-linear governing equation into an algebraic equation and then computes a solution through calculations using a computer^[9].

2.2 Detailed design

In the air current pulverizer, a rotating blade is assembled radially in an outer circumferential surface of the cylinder, which is integrated with the pulverizer at regular intervals, as shown in Fig. 1.

The cylinder in which the rotating blades are integrated is inserted into the outer circumferential surface of the rotating axis as shown in Fig. 2. A protruding portion is formed at the outer circumferential surface of the rotating axis and a groove, the shape of which corresponds to the protruding portion, is formed inside the cylinder. As a result, the durability of the pulverizing portion can be improved, the rotating blade can rotate at up to 8,000 rpm, and the material particles can be finely pulverized down to 3 μm .

The rotating blades are configured with two-layer portions: upper rotating blades where multiple blades are radially mounted and lower rotating blades that are mounted a certain distance away from the upper rotating blades. In addition, the upper and lower rotating blades are structured with two-layer blades: a pair of first and second blades. Each unit blade is radially mounted as shown in Fig. 3 and eight pairs of them are mounted.

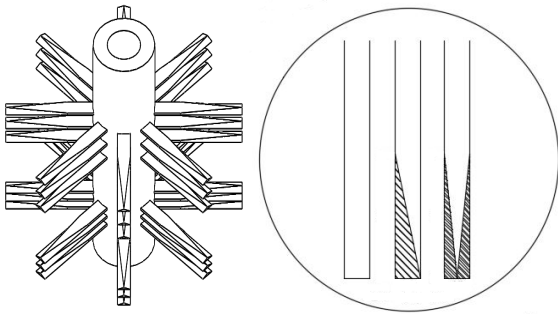


Fig. 1 Composition of wing blade units

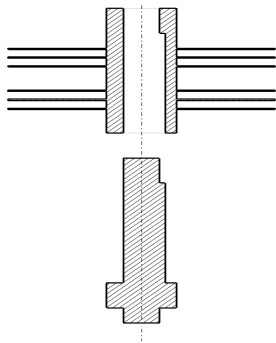


Fig. 2 Composition of a column units

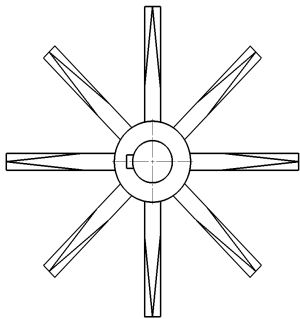


Fig. 3 Composition of a wing blade units

3. Verification of the Pulverizing Efficiency through CFD Analysis

3.1 Conceptual design of the pulverizing unit for CFD analysis

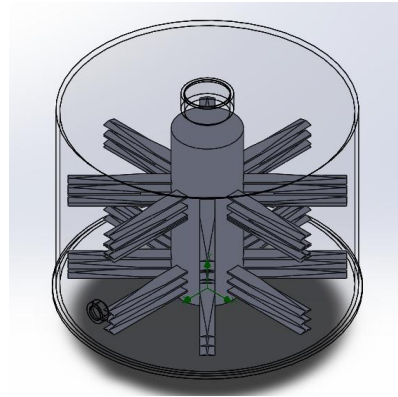


Fig. 4 Conceptual Design of Crushing Unit for Crushing Air Flow Analysis

Fig. 4 shows the 3D conceptual design of the pulverizing portion for airflow analysis. In the airflow pulverizer based on the detailed design in Fig. 6, the rotating blades are assembled radially in the cylinder's outer circumferential surface at regular intervals, as shown in Fig. 1. Then, the cylinder and pulverizer are integrated. The cylinder where the rotating blades are integrated is inserted into the outer circumferential surface of the rotating axis as shown in Fig. 4. The protruding portion is formed at the outer circumferential surface of the rotating axis and a groove, the shape of which corresponds with the protruding portion is formed inside the cylinder. Accordingly, when the cylinder in the center axis is rotated, the two-layer blades are rotated at a high speed and 3D modeling is performed to check the fluidity of the airflow phenomena, direction, distribution, and size.

Fig. 5 shows some of the results of CFD analysis according to the shape of the blade while rotating it at 3,200 rpm. The CFD analysis results exhibited that particle size distribution was uniform when the inclination was formed in the blade and the grinding efficiency was improved but also revealed that forming an inclination was not necessary in all blades.

3.2 Airflow analysis through CFD analysis

Fig. 6 shows the airflow, direction, and size according to the CFD analysis when the blade is rotating at 3,200 rpm. As shown in the results, the flow distribution was not constant and 83% of the fluid rates were <30 m/s. Fig. 7 - in which the blades rotated at 5,000 rpm - shows a somewhat improved fluid distribution flow but 60% of the fluid rates were <30 m/s and 13% of the rate distributions were 60 m/s. In addition, Fig. 8 - where the blades objects to be pulverized (grind target materials) settled on the bottom because the flow even occurred in the bottom layer. However, at 8,000 rpm in Fig. 8, the distribution of airflow particles was small in the bottom, which showed efficient pulverization.

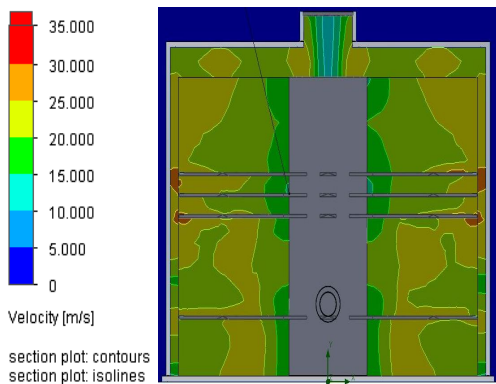


Fig. 5 Sectional Plot at 3200rpm of Crushing Unit

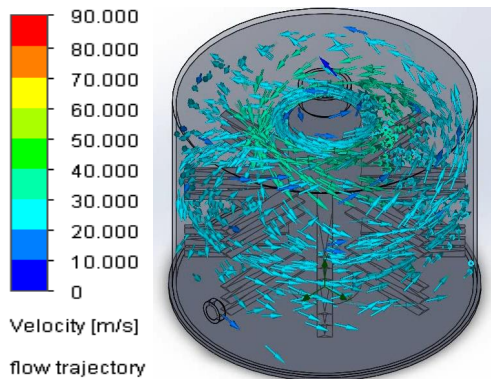


Fig. 6 Flow trajectory at 3,200 rpm of crushing unit

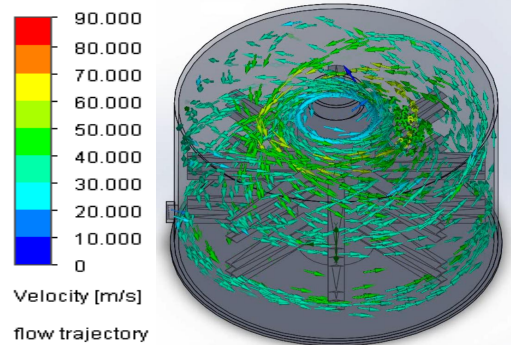


Fig. 7 Flow trajectory at 5,000 rpm of crushing unit

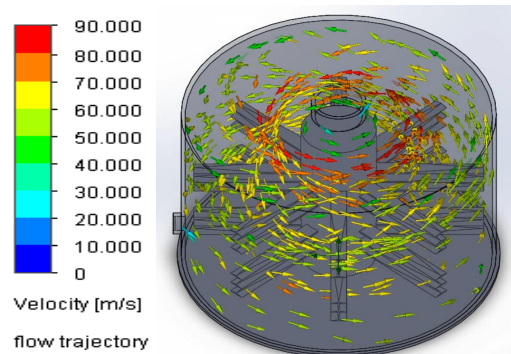


Fig. 8 Flow trajectory at 8,000 rpm of crushing unit

Table 1 Airflow velocity due to blade rotation

	Maximum speed	Lowest Speed	Average speed
3200rpm	30.38m/s	8.58m/s	22.96m/s
5000rpm	61.20m/s	12.85m/s	46.15m/s
8000rpm	103.24m/s	30.46m/s	72.69m/s

Table 2 experimental conditions for CFD analysis

Boundary condition	Other Setting Conditions
- Complete elastic reflection	- Fluid type: Air
- No thermal conduction	- Flow Type: Laminar and Turbulence
- Gravity and Rotation Impact	-Turbulent Strength: 0.1%
- Insulating wall	- Turbulence Length: 0.0031m
- Rotation Area: Blade Day Diameter and Axis Height	- Time: 10min
	- Humidity is not considered

3.3 Analysis of the particle distribution of pulverized objects

These are the experimental results when changing the shape and number of blades. If the configuration was set as shown above, the particle size distribution of the pulverized particles was uniform and the grinding efficiency was the highest. In addition, when the inclination was formed in the rotating blades, the particle size distribution of the pulverized particles was more uniform and the grinding efficiency was increased. However, there was no significant difference in particle size distribution or grinding efficiency between the two cases when the inclination was formed in all rotating blades or some of the rotating blades.

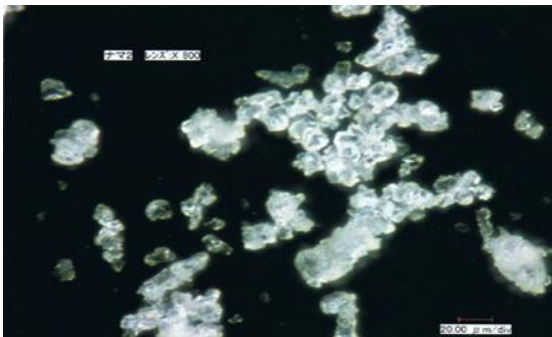


Fig. 9 Microscopic photograph of grain grinding particles caused by crushing unit

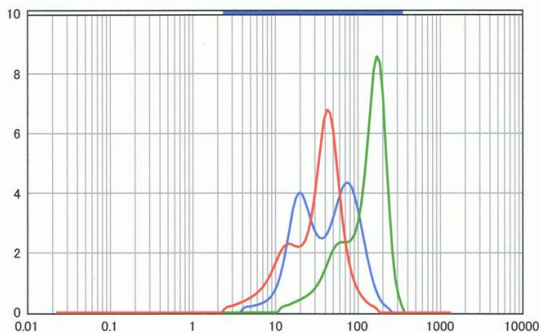


Fig. 10 Distribution for a crushing grit using the air current (red line)

Fig. 9 shows a micrograph of the pulverized grain particles. As shown in Fig. 9, the particles were relatively round and the particle size was in the range 3-20 μm , which showed the particle distribution was in the range 10-20 μm as shown in the measured results of Fig. 10.

The red line in Fig. 10 shows the particle distribution of the tested pulverized products at 8,000 rpm with the vane manufacturing of the pulverizer proposed in this study. As shown in this figure, the durability of the pulverizing portion can improve and the rotating blades can rotate at up to 8,000 rpm. The pulverizer can also finely grind particles of the grinding materials down to 3 μm and the average size of the particles was in the range 20-30 μm .

4. Conclusions

Conventional air current pulverizers have limited ability to increase the blade rotating speed beyond 4,000 rpm. In addition, they find it difficult to pulverize particles to $<30 \mu\text{m}$. In comparison, the integrated pulverizing device in this study can increase the speed of the rotating blade up to 8,000 rpm due to its structure. In addition, the pulverized particles can be as small as 3 μm due to the blade's integrated structure and the productivity per unit hour can be significantly improved. In particular, grains, nuts and various hard and brittle materials can be finely pulverized down to 3 μm by the structure of the rigid pulverizing device and super-fast rotation.

1. High-speed pulverization up to 8,000 rpm can be achieved because the principal axis was designed as key holder of the groove shape to enable high-speed rotation.
2. The analysis results after high-speed rotation at 3,200 rpm, 5,000 rpm, and 8,000 rpm of the principal axis verified that the double-bladed inclination was an efficient shape for the sloping

blade. In addition, they indicated that the productivity was improved and the distribution of particle sizes was uniform when the principal axis was rotated at 8,000 rpm.

3. The rotating blades can rotate at up to 8,000 rpm and the pulverizer can finely grind particles of grinding materials to 3 μm , where the average size of particles was in the range 20-30 μm .
4. Thus, when the same materials were used, the proposed pulverizer shows considerably lower production cost and maintenance and repair advantages.

References

1. Lee, M. G., Son S. H., Choung, M. G., Kim, S. T., Ko, J. M., Han, W. Y., Yoon, W. B., "Effect of Milling Methods and Particle Size on Rice Cake (Baeksulgi) Characteristics. Korean Society for Food Engineering," Journal of the Korean Society for Food Engineering Vol. 19, Issue. 1, pp. 1~7, 2015.
2. Ryu, B. M., Kim, C. S., "Impact of Milling Method on Quality Parameters of Waxy Sorghum Flour", Korean Society of Food and Cookery Science. Journal of the Korean Society of Food and Cookery Science, Vol. 29, Issue. 2, pp. 129~135, 2013.
3. Hirt, C. W. and Nichols, B. D., Volume of fluid (VOF) method for the dynamics of free boundaries, Journal of computational physics, Vol. 39, No. 1, pp. 201, 1981.
4. Kim, Y. H., Lee, S. K., "Solver for the Navier-Stokes Equations by using Initial Guess Velocity", Journal of KIISE: Computer Systems and Theory, Vol. 32, No. 9, pp. 445-456, 2005.
5. Atsushi U., Basic Course of Thermo-Fluid Analysis 15, 2019.
6. Henry, J., Ramos, M. A., "Factorization of boundary value problems using the invariant embedding method," Elsevier, 2016.
7. Du, L. X., Zeng, M., Wang, Q. W., "A Simplified CFD Model With Multi-Periodic Boundary Conditions for Cross Wavy Channels", In Turbo Expo: Power for Land, Sea, and Air, 2012.
8. Autodesk Inc.(2019), Periodic Boundary Condition <https://knowledge.autodesk.com/ko/support/cfd/learn-explore/caas/CloudHelp/cloudhelp/2019/KOR/SimCFD-UsersGuide/files/GUID-54B9C5DB-63E8-4D62-94FD-363FC46465C7-htm.html>
9. Autodesk Inc. discretization method, 2016. <https://knowledge.autodesk.com/ko/support/cfd/learn-explore/caas/CloudHelp/cloudhelp/2018/KOR/SimCFD-Learning/files/GUID-DEE0664D-771B-4446-9ED4-1498267D13FB-htm.html>
10. Kim, G. H., "Optimal Shape Design of ANG Fuel Vessel Applied to Composite Carbon Fiber," Journal of the Korean Society of Manufacturing Process Engineers, Vol. 18, No. 1, pp. 65-71, 2019.
11. Kim, G. H., Manufacturing of Apparatus for Producing Stream Crushing Units, Project Report LINC+, pp. 5-45, 2019.
12. GV, GV-CNC Users Manual, Cubictek do., ltd, pp. 97-118, 2018.
13. Lee, H. S., Na, Y. M., Jang, H. S., Suk, I. H., Kang, S. H., Kim, H. J., Park, J. K., "A Study on the Stability of Shield TBM Thrust Jack in the Behavior of Operating Fluid According to Thrust Force", Journal of the Korean Society of Manufacturing Process Engineers Vol. 18, No. 1, pp. 38-45, 2019.
14. Yoon, H. Y., Jeon, G. H., Choi, J. Y., "A Study on the Design of Transmission Oil-Seal Using 2D Finite Element Analysis", Journal of the Korean Society of Manufacturing Process Engineers Vol. 18, No. 1, pp. 85-93, 2019.